Antiferromagnetic phase transition in garnet-type AgCa2Co2V3012 and AgCa2Ni2V3012

著者	AWAKA Junji, ITO Masakazu, SUZUKI Takashi, NAGATA Shoichi
journal or publication title	Journal of physics and chemistry of solids
volume	66
number	5
page range	851-860
year	2005-05
URL	http://hdl.handle.net/10258/346

doi: info:doi/10.1016/j.jpcs.2004.11.006

Antiferromagnetic phase transition in garnet-type $AgCa_2Co_2V_3O_{12}$ and $AgCa_2Ni_2V_3O_{12}$

Junji Awaka[a], Masakazu Ito[b], Takashi Suzuki[b], Shoichi Nagata[a,*]

[a]*Department of Materials Science and Engineering, Muroran Institute of Technology, 27-1 Mizumoto-cho, Muroran, Hokkaido 050-8585, Japan*

[b]*Department of Quantum Matter, Graduate School of Advanced Science of Matter, Hiroshima University, Higashi-hiroshima, 739-8526, Japan*

Abstract

Antiferromagnetic phase transition in two vanadium garnets $AgCa_2Co_2V_3O_{12}$ and $AgCa_2Ni_2V_3O_{12}$ has been found and investigated extensively. The heat capacity exhibits sharp peak due to the antiferromagnetic order with the Néel temperature T_N = 6.39 K for $AgCa_2Co_2V_3O_{12}$ and 7.21 K for $AgCa_2Ni_2V_3O_{12}$, respectively. The magnetic susceptibility exhibit broad maximum, and these T_N correspond to the inflection points of the magnetic susceptibility χ a little lower than $T(\chi_{max})$. The magnetic entropy changes from zero to 20 K per mol Co^{2+} and Ni^{2+} ions are 5.31 J K^{-1}mol-Co^{2+}-ion^{-1}and 6.85 J K^{-1} mol-Ni^{2+}-ion^{-1}, indicating S = 1/2 for Co^{2+} ion and S = 1 for Ni^{2+} ion. The magnetic susceptibility of $AgCa_2Ni_2V_3O_{12}$ shows the Curie-Weiss behavior between 20 and 350 K with the effective magnetic moment μ_{eff} = 3.23 μ_B Ni^2-ion^{-1} and the Weiss constant θ = –16.4 K.The simple Curie-Weiss law can not be applicable for $AgCa_2Co_2V_3O_{12}$. The complex temperature dependence of magnetic susceptibility has been interpreted within the framework of Tanabe-Sugano energy diagram, which is analyzed on the basis of crystalline electric field. The ground state is the spin doublet state ^2E (t_2^6e) and the first excited state is spin quartet state $^4T_1$ ($t_2^5e^2$) which locates extremely close to the ground state. The low spin state S = 1/2 for Co^{2+} ion is verified experimentally at least below 20 K which is in agreement with the result of the heat capacity.

Keywords: A. Inorganic compounds; A. Oxides; D. Magnetic properties; D. Crystal fields; D. Specific heat

---

*Corresponding author. Fax : +81-143-46-5612.

E-mail address : naga-sho@mmm.muroran-it.ac.jp (S. Nagata)

1. Introduction

The garnet-type compounds have been attracting great interests on the magnetic properties in the theory and experiments, in particular, ferrimagnetism of rare earth iron garnets $R_3Fe_5O_{12}$ [1]. Fig. 1 shows the garnet structure has cubic symmetry with space group $Ia\bar{3}d$ (No. 230). The general chemical formula of the oxide garnet may be written as $\{C\}_3[A]_2(D)_3O_{12}$, where *C*, *A*, and *D*-sites are the cation sites. These cation sites are surrounded by oxygen ions O^{2-} at dodecahedron, octahedron, and tetrahedron, respectively. Many investigations have been made for the garnets with magnetic ions distributed over *C, A, D*-three or two sublattices. Garnets having only one magnetic sublattice are diluted magnetic system and are of interest as a simpler system.

When the *D*-site is occupied by V^{5+} ion, so called vanadium garnet (V-garnet), many works were made mainly by Russian researches nearly 30 years ago [2-13], where detailed analysis has not been presented for the magnetic properties. These V-garnets can provide the diluted magnetic system or non-magnetic system. The V-garnets of $AgCa_2Co_2V_3O_{12}$ and $AgCa_2Ni_2V_3O_{12}$ are synthesized by Ronniger *et al*. [9], where only the lattice constants are given. No physical property has been measured so far.

We have also successfully synthesized high purity V-garnets of $AgCa_2Co_2V_3O_{12}$ and $AgCa_2Ni_2V_3O_{12}$ and $AgCa_2Zn_2V_3O_{12}$, where $AgCa_2Zn_2V_3O_{12}$ is non-magnetic and then used as a standard compounds without magnetic properties. In these compounds, ionic distributions are $\{AgCa_2\}[Co_2](V_3)O_{12}$ and $\{AgCa_2\}[Ni_2](V_3)O_{12}$ and $\{AgCa_2\}[Zn_2](V_3)O_{12}$. Ag^+ and Ca^{2+} ions occupy *C*-site, Co^{2+}, Ni^{2+} or Zn^{2+} ions occupy *A*-site and V^{5+} ions occupy *D*-site. Here these Co^{2+} and Ni^{2+} ions at *A*-site are only magnetic and the other ions have closed shell with non-magnetic state. The studies of the synthesis and crystallographic refinement by the Rietveld method for $AgCa_2Co_2V_3O_{12}$ and $AgCa_2Ni_2V_3O_{12}$ have been published in our previous report [14]. We have measured the heat capacity and the magnetic susceptibility of V-garnets. The antiferromagnetic Néel order have first found with $T_N = 6.39$ K for $AgCa_2Co_2V_3O_{12}$ and 7.21 K for $AgCa_2NI_2V_3O_{12}$. In addition, the antiferromagnetic ordered state has not been observed down to 4.2 K for $AgCa_2Cu_2V_3O_{12}$ [15]. The Néel temperature could be below 1 K. In this paper, the experimental results of thermal and magnetic properties for $AgCa_2Co_2V_3O_{12}$ and $AgCa_2Ni_2V_3O_{12}$ have been analyzed in details within the frame work of Tanabe-Sugano energy diagram.

The particular emphasis and attention are paid to the significant difference between Co^{2+} and Ni^{2+} ions at octahedron *A*-site under the influence of crystalline electric field (CEF). The free ions of Co^{2+} ($3d^7$) and Ni^{2+} ($3d^8$) ions have an orbital *F* state ($L = 3$) as ground state. For Co^{2+} ion, there remains Kramer's degeneracy, therefore the correlation between CEF and the spin-orbit interaction is more complicated in comparison with Ni^{2+} ion system. This paper will present the difference of the magnetic state between $\{AgCa_2\}[Co_2](V_3)O_{12}$ and $\{AgCa_2\}[Ni_2](V_3)O_{12}$ and will provided. The magnetic susceptibility of $AgCa_2Ni_2V_3O_{12}$ shows the Curie-Weiss behavior between 20 and 350 K with the effective magnetic moment $\mu_{eff} = 3.23\ \mu_B$ Ni^{2+}-ion^{-1}. The magnetic susceptibility result of $AgCa_2Co_2V_3O_{12}$ shows the complex temperature dependence. We discuss this result on the basis of the idea that the excited state influences significantly the magnetic susceptibility, arising from the presence of a thermally accessible high-spin state lying above the low-spin ground state. The knowledge of CEF enables us to understand the complex temperature dependence of the magnetic susceptibility for $AgCa_2Co_2V_3O_{12}$, which will be discussed below.

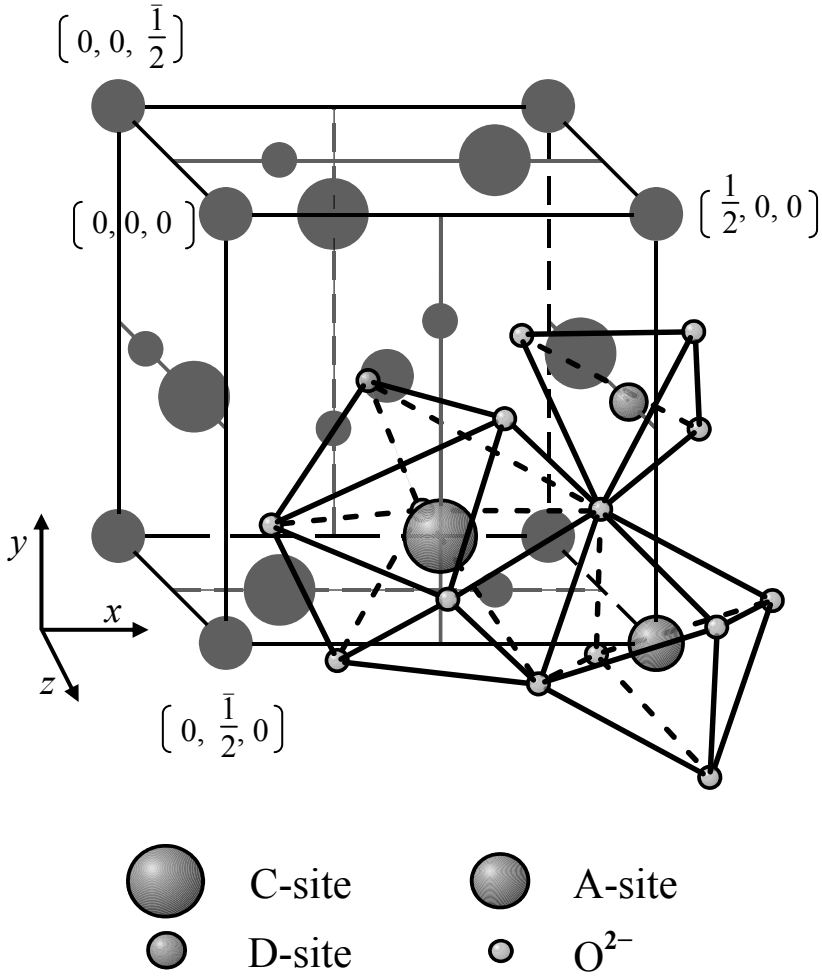

Fig. 1. An eighth of unit cell of garnet-type structure $\{C\}_3[A]_2(D)_3O_{12}$ with the different sites *C*, *A* and *D*.

2. Experimental methods

Powder specimens of $AgCa_2Co_2V_3O_{12}$, $AgCa_2Ni_2V_3O_{12}$ and $AgCa_2Zn_2V_3O_{12}$ were prepared through a solid-state chemical reaction. The synthesis and detailed crystallographic studies of $AgCa_2Co_2V_3O_{12}$ and $AgCa_2Ni_2V_3O_{12}$ have been recently made on the basis of the Rietveld analysis in which the refined structure parameters are presented [14]. The synthesis and magnetic property studies of $AgCa_2Zn_2V_3O_{12}$ have been published on ref. [15]. The heat capacity was measured with a Quantum Design PPMS Heat Capacity Option (HC) Model P650 over the temperature range 0.42 to 60 K in zero field. The dc magnetic susceptibility χ of powder specimen was measured with a Quantum Design superconducting quantum interference device (MPMS, *rf*-SQUID) magnetometer over the temperature range 2.0 to 350 K under zero field cooled (ZFC) and field cooled (FC) conditions.

3. Results and discussion

3.1 *Heat capacity*

3.1.1 *Lattice heat capacity*

Fig. 2 depicts the molar (formula-unit) heat capacity C as a function of temperature over the range 0.42 to 40 K. Two compounds of $AgCa_2Co_2V_3O_{12}$ and $AgCa_2Ni_2V_3O_{12}$ exhibit a sharp peak due to the antiferromagnetic phase transition at 6.39 K and 7.21 K, respectively.

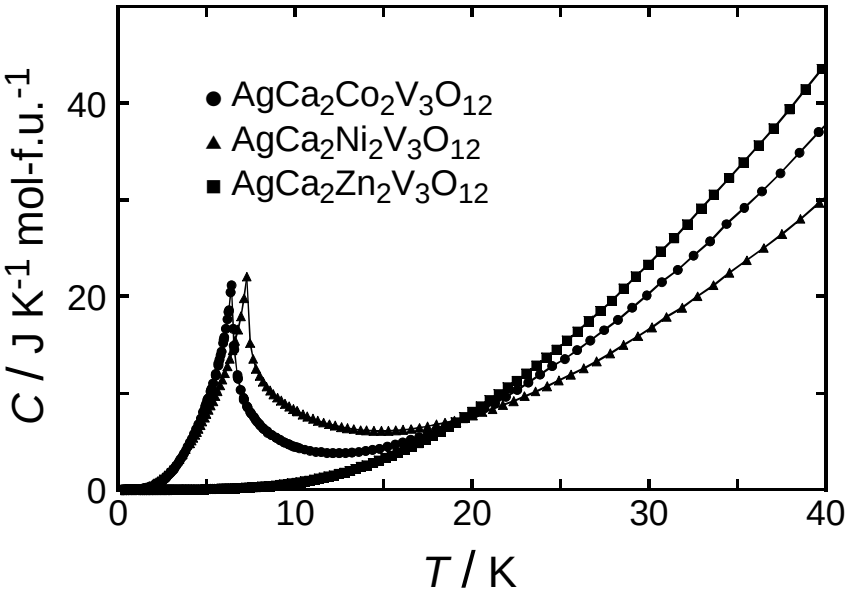

Fig. 2. Measured heat capacity of vanadium garnets as a function of the temperature.

On the other hand $AgCa_2Zn_2V_3O_{12}$ is non-magnetic and then C does not indicate any magnetic anomaly but only the lattice heat capacity C_{lattice}. The magnitude of the heat capacity in Fig. 2 for three compounds is fairly same around 20 K and the experimental values grow rapidly above 20 K. It is noted that the molar weights are 650.71 g mol^{-1} for $AgCa_2Co_2V_3O_{12}$, 650.23 g mol^{-1} for $AgCa_2Ni_2V_3O_{12}$ and 663.66 g mol^{-1} for $AgCa_2Zn_2V_3O_{12}$; the order of the value of C_{lattice} for three compounds is reasonable. The curve of $AgCa_2Zn_2V_3O_{12}$ in Fig. 2 shows C_{lattice}, following the Debye T^3 approximation.

$$C_{\text{lattice}} = \left(\frac{12}{5}\right)\pi^4 N_{\text{A}} k_{\text{B}} r \left(\frac{T}{\Theta_{\text{D}}}\right)^3 = 1943.8 r \left(\frac{T}{\Theta_{\text{D}}}\right)^3 \quad (1)$$

where N_A is the Abogadro's number, k_B the Boltzmann's constant, Θ_D the Debye temperature, T the temperature and r the number of atoms per formula unit, which is found to be r = 20 for garnet compound. Fig. 3 is the Debye T^3 approximation of low temperature lattice heat capacity for $AgCa_2Zn_2V_3O_{12}$ as a function of the temperature. The Debye temperature Θ_D is obtained to be 410 K (r = 20) and 151 K (r = 1).

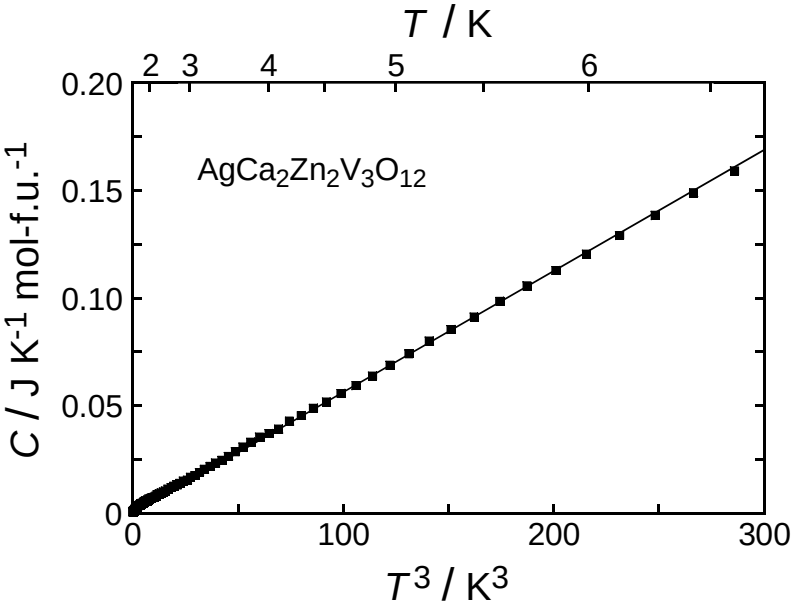

Fig. 3. The Debye T^3 approximation of low temperature lattice heat capacity for $AgCa_2Zn_2V_3O_{12}$.

The accurate subtraction of the lattice contribution from the total heat capacity of $AgCa_2Co_2V_3O_{12}$ and $AgCa_2Ni_2V_3O_{12}$ is a rather serious problem. Here we subtracted $C_{lattice}$ by using the experimental value of the $AgCa_2Zn_2V_3O_{12}$. Furthermore we adopted the molecular mass correction using the following relation,

$$C'_{\text{lattice}} = \left(\frac{M'}{M}\right)^{\frac{3}{2}} C_{\text{lattice}}, \qquad (2)$$

where $C_{lattice}$ is the lattice heat capacity of $AgCa_2Zn_2V_3O_{12}$, and the $C'_{lattice}$ is the hypothesized lattice heat capacity of $AgCa_2Co_2V_3O_{12}$ or $AgCa_2Ni_2V_3O_{12}$, as if these $AgCa_2Co_2V_3O_{12}$ and $AgCa_2Ni_2V_3O_{12}$ would be just non-magnetic compounds. The values of $(M'/M)^{3/2}$ are 9.71×10^{-1} for $AgCa_2Co_2V_3O_{12}$ and 9.70×10^{-1} for $AgCa_2Ni_2V_3O_{12}$.

3.1.2 *Nuclear Zeeman effect of the heat capacity for cobalt nucleus*

The experimental value of the heat capacity for $AgCa_2Co_2V_3O_{12}$ exhibits the slight increase with decreasing temperature below 0.7 K, while this increase was not found in the heat capacity of $AgCa_2Ni_2V_3O_{12}$ at low temperature. In Fig. 4, the solid circles show the heat capacity of $AgCa_2Co_2V_3O_{12}$ after the subtraction of the lattice contribution. We presume this increase of the heat capacity of $AgCa_2Co_2V_3O_{12}$ indicates the tail of the nuclear spin heat capacity C_{nuclear} due to the nuclear Zeeman effect of Co nucleus with I = 7/2. The nuclear spin I = 7/2 of ^{59}Co has 100 % natural abundance, while ^{61}Ni nucleus has I = 3/2 but low 1.1399 % natural abundance and therefore negligibly small effect. Therefore, Co nucleus with I = 7/2 is influenced strongly by the internal field due to the electron moment arisen from the antiferromagnetic order of Co^{2+} ion below T_N = 6.39 K. In the temperature range 0.42 to 0.49 K, C versus $1/T^2$ plot follows in a straight line, where C indicates the heat capacity after the subtraction of C_{lattice}.

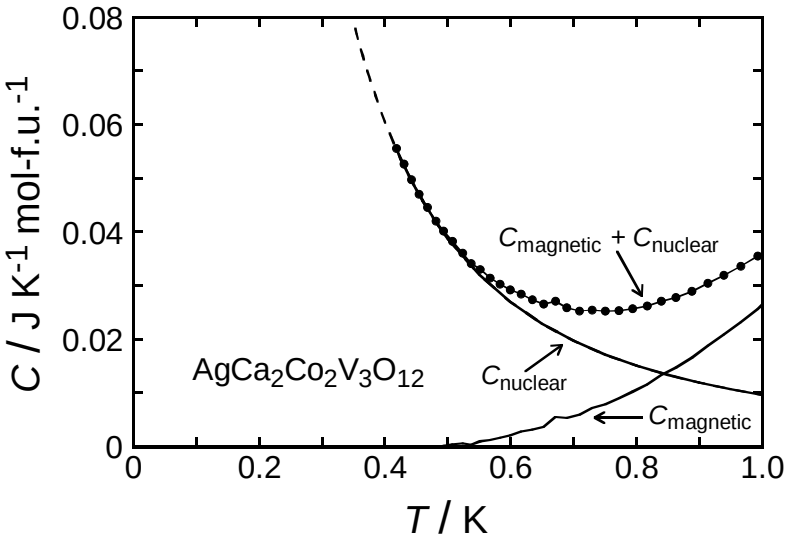

Fig. 4. The expanded plot of the low temperature heat capacity of $AgCa_2Co_2V_3O_{12}$ after the subtraction of lattice contribution. The nuclear Zeeman effect heat capacity for Co nucleus and magnetic heat capacity for Co^{2+} ion are overlapped. Here, the magnetic heat capacity of Co^{2+} ion is calculated from the value of experimental result minus nuclear Zeeman effect, see text.

Fig. 4 represents the expanded plot of low temperature heat capacity of $AgCa_2Co_2V_3O_{12}$ which consists of two parts with C_{nuclear} and the magnetic heat capacity C_{magnetic} originated from Co^{2+} ion. The solid curve of C_{nuclear} indicates the extrapolated result assuming $1/T^2$ form and the C_{magnetic} indicates calculated results of $C - C_{\text{nuclear}}$.

Let us calculate the nuclear Zeeman heat capacity under the internal magnetic field due to the Co^{2+} ion. The partition function Z of the nuclear Zeeman split for Co nucleus with I = 7/2 is

$$Z = \sum_j g_j \exp\left(-\frac{\varepsilon_j}{k_B T}\right) = 2\sum_{j=1}^{4} \cosh\left(\frac{2j-1}{2}\frac{\Delta}{k_B T}\right), \tag{3}$$

where g_j is the degree of degeneracy, ε_j the energy, Δ the difference between the each energy level, here the origin of the energy is assumed to be the center of width of the Zeeman splitting. The internal energy U is

$$U = \frac{N}{Z}\sum_j \varepsilon_j \exp\left(-\frac{\varepsilon_j}{k_B T}\right)$$

$$= -\frac{\Delta N}{Z}\sum_{j=1}^{4}(2j-1)\sinh\left(\frac{2j-1}{2}\frac{\Delta}{k_B T}\right), \tag{4}$$

where N is the number of magnetic ions. The nuclear spin Zeeman heat capacity at constant volume of Co nucleus is given by,

$$C_{\text{nuclear}} = \left(\frac{\partial U}{\partial T}\right)_{\text{v}} ,$$

$$= \left(\frac{\Delta}{k_B T}\right)^2 \frac{N k_B}{Z^2}(A - B) ,$$

$$A = \left\{\sum_{j=1}^{4}(2j-1)^2 \cosh\left(\frac{2j-1}{2}\frac{\Delta}{k_B T}\right)\right\}\left\{\sum_{j=1}^{4}\cosh\left(\frac{2j-1}{2}\frac{\Delta}{k_B T}\right)\right\}$$
$$B = \left\{\sum_{j=1}^{4}2(2j-1)\sinh\left(\frac{2j-1}{2}\frac{\Delta}{k_B T}\right)\right\}\left\{\sum_{j=1}^{4}\frac{2j-1}{2}\sinh\left(\frac{2j-1}{2}\frac{\Delta}{k_B T}\right)\right\}. \tag{5}$$

The asymptotic form of C_{nuclear} at higher temperature is obtained in terms of $1/T^2$ as $k_B T >> \Delta$,

$$C_{\text{nuclear}} \approx \frac{21}{4}\left(\frac{\Delta}{k_B T}\right)^2 N k_B \qquad (k_B T >> \Delta). \tag{6}$$

The value Δ is estimated to be 5.17 tesla (10.6 mK, 1.46×10^{-25} J) in comparison

with the formula (6) and the experimental result. Fig. 5 shows the calculated result of the heat capacity due to the nuclear Zeeman effect of Co nucleus in $AgCa_2Co_2V_3O_{12}$. The peak is 10.8 mK, and maximum value of $C_{nuclear}$ is about 15.0 J K^{-1} mol-f.u.$^{-1}$.

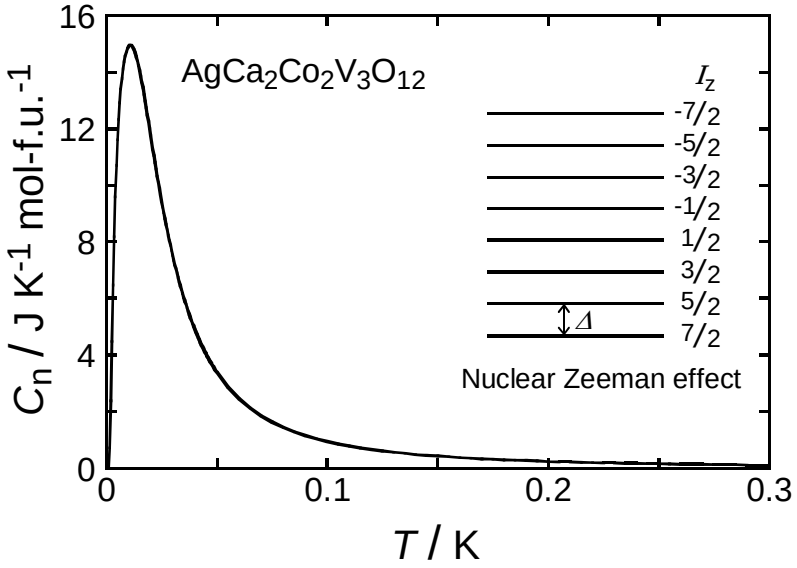

Fig. 5. Nuclear Zeeman effect of Co^{2+} ion in $AgCa_2Co_2V_3O_{12}$. Nuclear spin heat capacity as a function of the temperature at low temperature.

3.1.3 *Antiferromagnetic heat capacity*

Fig. 6 shows the temperature dependence of the magnetic heat capacity $C_{magnetic}$ of $AgCa_2Co_2V_3O_{12}$ and $AgCa_2Ni_2V_3O_{12}$ coming from the electron spin. These magnetic heat capacities are obtained after the subtraction; $C_{magnetic} = C - C_{lattice} - C_{nuclear}$ for $AgCa_2Co_2V_3O_{12}$ and $C_{magnetic} = C - C_{lattice}$ for $AgCa_2Ni_2V_3O_{12}$, where C indicates the total heat capacity measured experimentally. The sharp peak corresponds to the Néel temperature T_N which is 6.39 K for $AgCa_2Co_2V_3O_{12}$ and 7.21 K for $AgCa_2Ni_2V_3O_{12}$. Fig. 7 displays the magnetic heat capacity in the narrow temperature region over 4.0 to 9.0 K around T_N. The magnetic enthalpy $E_{magnetic}$ is evaluated by

$$E_{magnetic} = \int_0^T C_{magnetic} dT \quad . \tag{7}$$

The values of $E_{magnetic}$ over the temperature range zero to 20 K are 34.9 J mol-Co^{2+}-ion^{-1} for $AgCa_2Co_2V_3O_{12}$ and 50.9 J mol-Ni^{2+}-ion^{-1} for $AgCa_2Ni_2V_3O_{12}$.

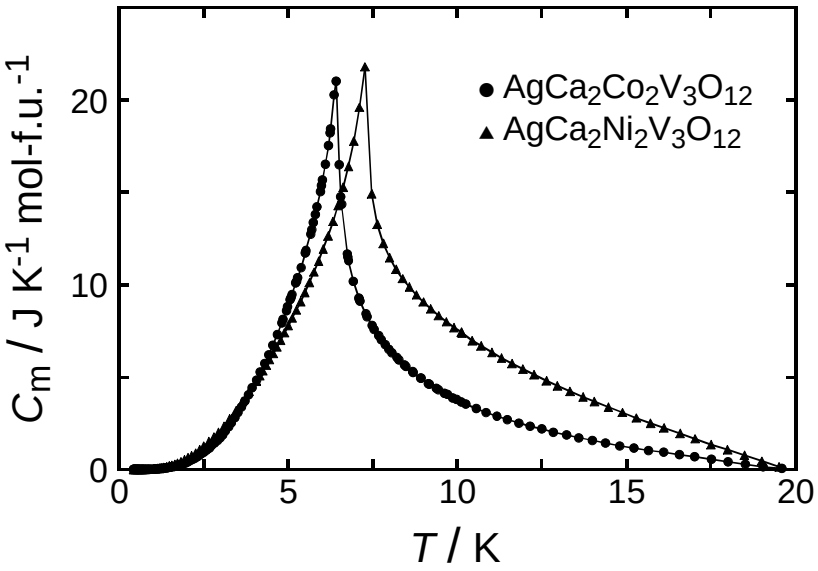

Fig. 6. Magnetic heat capacity of $AgCa_2Co_2V_3O_{12}$ and $AgCa_2Ni_2V_3O_{12}$ a function of the temperature. The Néel temperature is 6.39 K for $AgCa_2Co_2V_3O_{12}$ and 7.21 K for $AgCa_2Ni_2V_3O_{12}$.

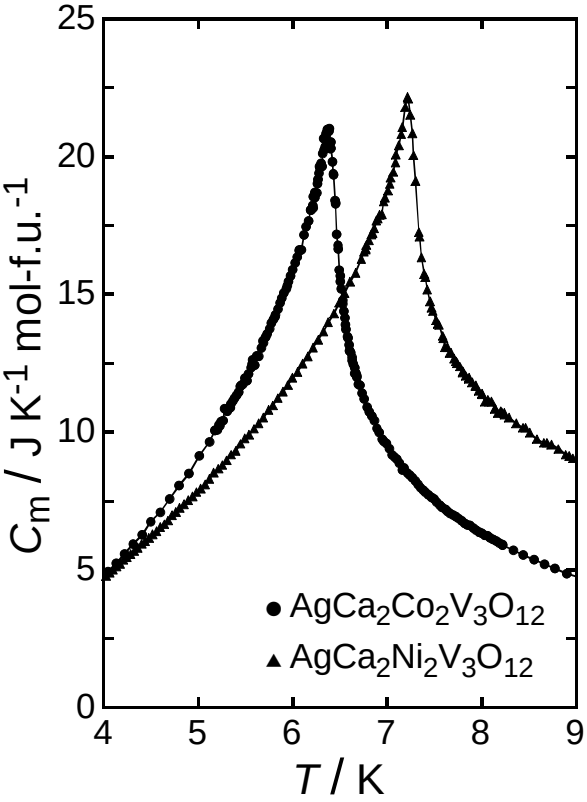

Fig. 7. The expanded plot of the magnetic heat capacity around the Néel temperature.

Fig. 8 indicates the temperature dependence of C_{magnetic}/T for $AgCa_2Co_2V_3O_{12}$ and $AgCa_2Ni_2V_3O_{12}$. The experimental observation of the magnetic entropy change S_{magnetic} over the temperature range zero to 20 K is presented in Fig. 9 using the following expression,

$$S_{\text{magnetic}} = \int_0^T \frac{C_{\text{magnetic}}}{T}\, dT \ . \tag{8}$$

Fig. 9 depicts the magnetic entropy S_{magnetic}/mol-magnetic-ion of $AgCa_2Co_2V_3O_{12}$ and $AgCa_2Ni_2V_3O_{12}$ as a function of the temperature. The total magnetic entropy change $\Delta S_{\text{magnetic}}$/mol-magnetic-ion is 5.31 J K^{-1} mol-Co^{2+}-ion^{-1} for $AgCa_2Co_2V_3O_{12}$ and 6.85 J K^{-1} mol-Ni^{2+}-ion^{-1} for $AgCa_2Ni_2V_3O_{12}$. The calculated entropy change $\Delta S_{\text{magnetic}}$/mol-ion is 5.76, 9.13 and 11.5 J K^{-1} mol-ion^{-1}, for the value of spin S = 1/2, 1 and 3/2; further, the values in the unit of $\Delta S_{\text{magnetic}}/R = \ln(2S + 1)$ per mol-ion are 0.693, 1.10 and 1.39, respectively, R is the gas constant. It is stressed that the experimental result of entropy change supports the spin value of S = 1/2 for Co^{2+} ion in $AgCa_2Co_2V_3O_{12}$. As for Ni^{2+} ion in $AgCa_2Ni_2V_3O_{12}$, the experimental value is a little less than that of expected value for S = 1, where the origin of this difference may come from the overestimation of the lattice heat capacity. The ratio of the magnetic entropy change below and above T_N is evaluated to be $\Delta S_{\text{magnetic}}(T<T_N)$ = 58 % and $\Delta S_{\text{magnetic}}(T>T_N)$ = 42 % for $AgCa_2Co_2V_3O_{12}$; $\Delta S_{\text{magnetic}}(T<T_N)$ = 60 % and $\Delta S_{\text{magnetic}}(T>T_N)$ = 40 % for $AgCa_2Ni_2V_3O_{12}$.

The A-site sublattice consists of bcc structure where the magnetic interactions between each magnetic ion are fairly complicated. It should be noticed that the strong short-range order (SRO) effect has been observed in these two garnets of $AgCa_2Co_2V_3O_{12}$ and $AgCa_2Ni_2V_3O_{12}$. Figs. 6 and 7 show the not λ-type anomaly of the heat capacity but rather symmetrical shape between below and above T_N in narrow temperature region, which is one of the typical characteristics of low-dimensional magnetic phase transition. Fig. 9 also demonstrates the SRO effect which indicates that the magnetic entropy change above T_N is approximately 40 % for both garnets. The magnetic ions at A-site are separated in series by at least two O^{2-} ions from the nearest neighbor magnetic one. The magnetic interaction is rather novel. As a consequence the theory of superexchange coupling interaction can not be applicable to understand these V-garnet systems. The determination of the magnetic structure is great significant, which will be the coming issue of these compounds. The substantial amount of magnetic dipole-dipole interaction may be not completely neglected in this system because the number of the nearest neighbor of magnetic ion is 8 and next n.n. is 6. The spin wave excitation of the three-dimensional antiferromagnetic system predicts T^3 law of C_{magnetic} at low temperature. Figs. 10 and 11 show a T^3 plots of C_{magnetic} for $AgCa_2Co_2V_3O_{12}$ and $AgCa_2Ni_2V_3O_{12}$. The experimental data is fairly in agreement with the theoretical predictionof T^3 law over the temperature range 0.42 to 5.85 K for $AgCa_2Co_2V_3O_{12}$ and 0.42 to 3.27 K for $AgCa_2Ni_2V_3O_{12}$. Once these compounds undergo the long-range order on passing below T_N, the three-dimensional interaction is established firmly and then the spin wave excitation of the three-dimensional antiferromagnetic system with T^3 law can be expected.

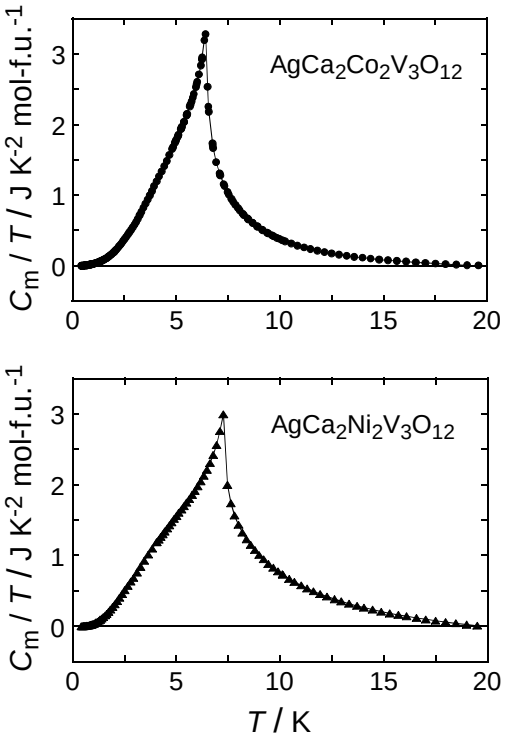

Fig. 8. $C_{magnetic}/T$ versus T plots for $AgCa_2Co_2V_3O_{12}$ and $AgCa_2Ni_2V_3O_{12}$.

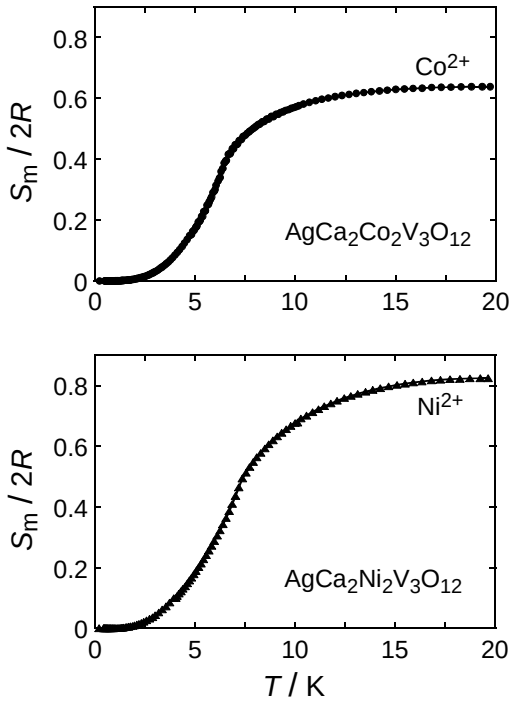

Fig. 9. Magnetic entropy of $AgCa_2Co_2V_3O_{12}$ and $AgCa_2Ni_2V_3O_{12}$ as a function of the temperature. The unit of the vertical axis is defined to be magnetic entropy per mol-magnetic-ion.

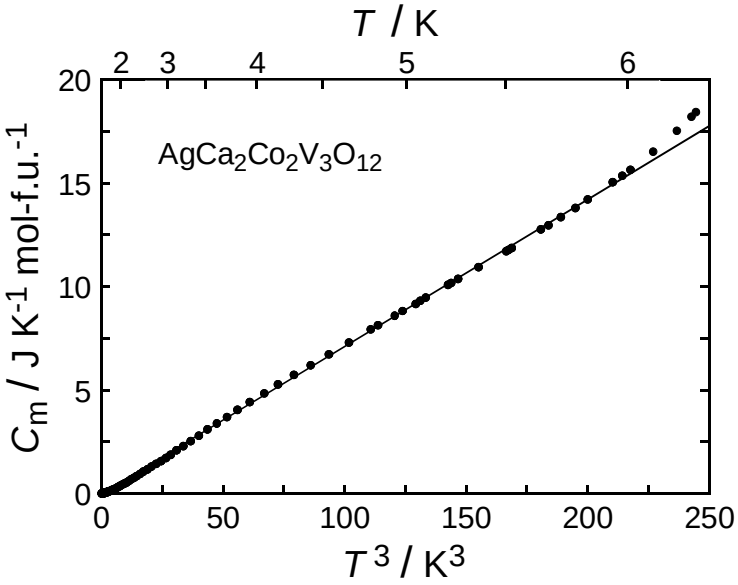

Fig. 10. Magnetic heat capacity versus T^3 for $AgCa_2Co_2V_3O_{12}$ on the basis of antiferromagnetic spin wave excitation.

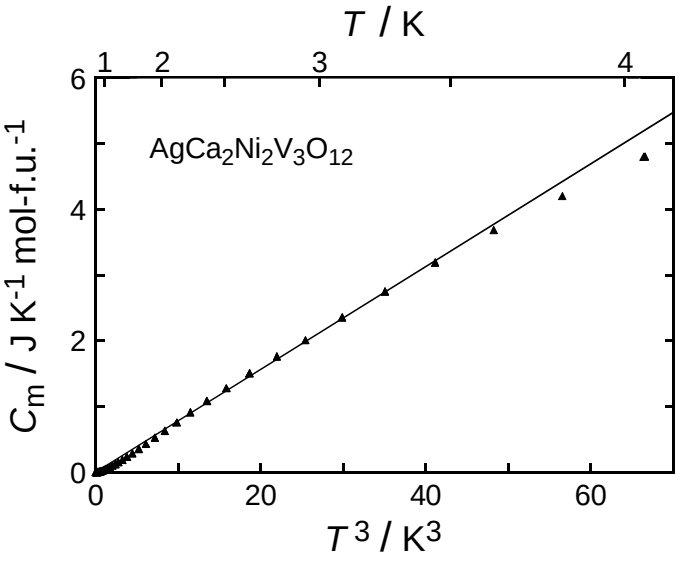

Fig. 11. Magnetic heat capacity versus T^3 for $AgCa_2Ni_2V_3O_{12}$ on the basis of antiferromagnetic spin wave excitation.

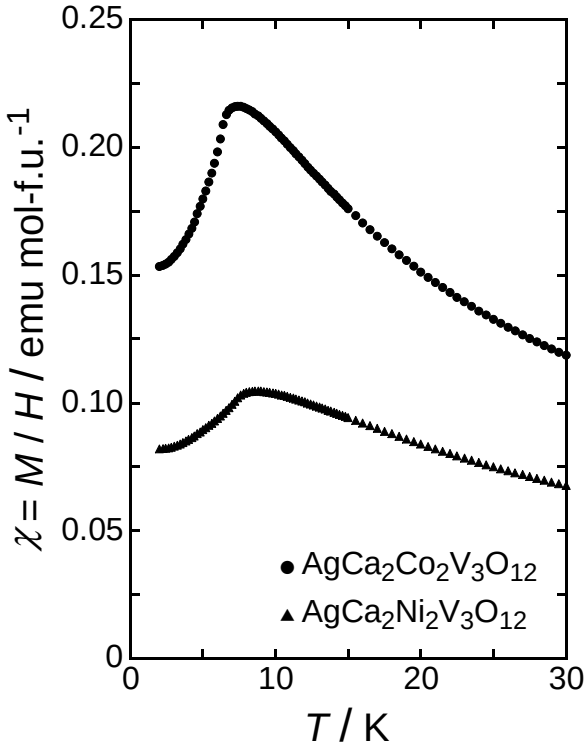

Fig. 12. Magnetic susceptibilities χ for $AgCa_2Co_2V_3O_{12}$ and $AgCa_2Ni_2V_3O_{12}$ as a function of temperature, obtained in an applied field of 1.00 kOe under zero-field cooled condition.

3.2 *Magnetic susceptibility*

3.2.1 *$AgCa_2Ni_2V_3O_{12}$*

Fig 12 shows the temperature dependence of the magnetic susceptibility χ in an applied field H of 1.00 kOe for $AgCa_2Co_2V_3O_{12}$ and $AgCa_2Ni_2V_3O_{12}$. The susceptibility is caused by localized magnetic moment of Co^{2+} ion and Ni^{2+} ion and has antiferromagnetic order with round maximum of χ_{max} with the temperatures of 7.40 K and 8.80 K, respectively. The values of χ(2.0 K)/χ_{max} are 0.71 for $AgCa_2Co_2V_3O_{12}$ and 0.78 for $AgCa_2Ni_2V_3O_{12}$ which are a little larger than 2/3 expected for antiferromagnets for the powder specimen. Fig. 13 presents the temperature derivative of χ as a function of the temperature. This peak temperature of $d\chi/dT$ corresponds to that at the sharp peak of the heat capacity, defining the Néel temperature. It is noted that the temperature of round maximum of χ_{max} is not in agreement with T_N observed in the heat capacity.

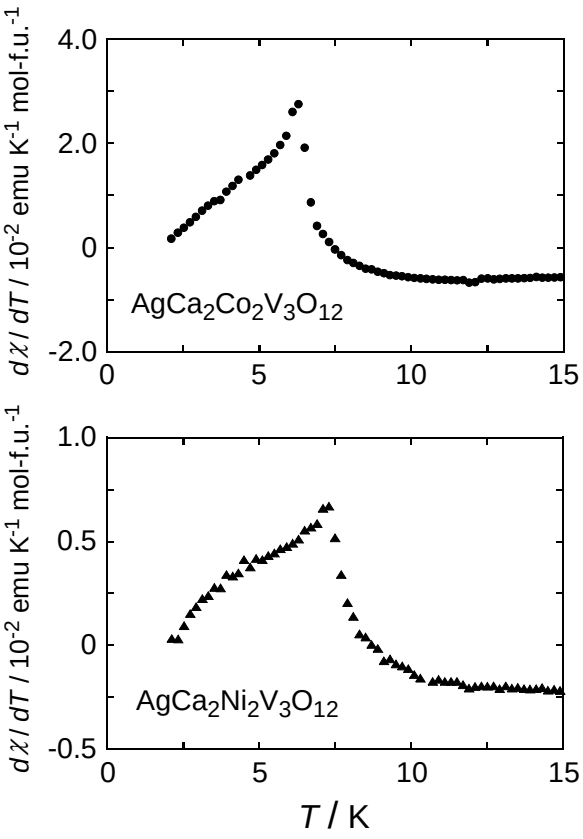

Fig. 13. Temperature derivative of χ as a function of temperature, using tha data of Fig. 12. This peak temperature of $d\chi/dT$ corresponds to that at the sharp peak of the heat capacity, indicating Néel temperature.

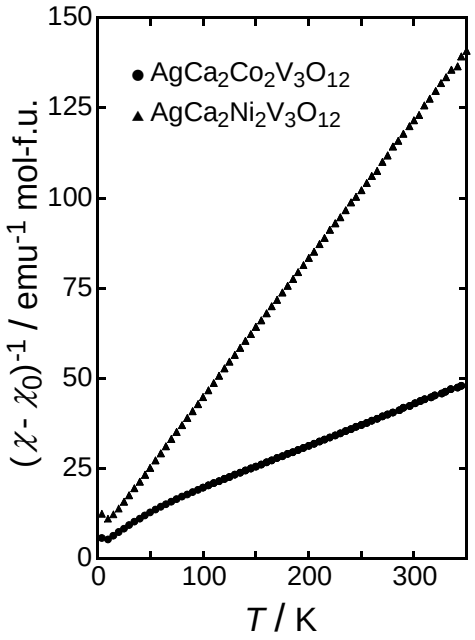

Fig. 14. Inverse magnetic susceptibility as a function of temperature in a constant magnetic field of 10.0 kOe. The solid circle shows $AgCa_2Co_2V_3O_{12}$ and the solid triangle shows $AgCa_2Ni_2V_3O_{12}$.

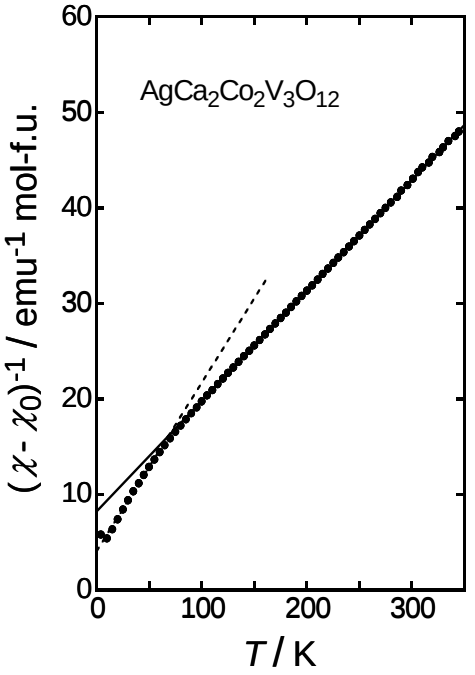

Fig. 15. The expanded plot of the inverse susceptibility in a constant magnetic field of 10.0 kOe for $AgCa_2Co_2V_3O_{12}$. The solid line shows a fit over the high temperature range 100 to 350 K and the dotted line shows the lower temperature region 20 to 60 K.

The inverse magnetic susceptibility in an applied magnetic field H of 10.0 kOe is indicated in Fig. 14. The susceptibility of $AgCa_2Ni_2V_3O_{12}$ is well described over the temperature range 20 to 350 K by a modified Curie-Weiss law,

$$\chi = \frac{C}{T-\theta} + \chi_0, \tag{9}$$

where C is the Curie constant, θ the Curie-Weiss θ and χ_0 a temperature independent term, T the temperature. The experimental result of χ_0 is found to be 3.16×10^{-3} emu mol-f.u.$^{-1}$. The amount of diamagnetic contribution caused by the atomic core electrons χ_{dia} for $Ag^+ + 2Ca^{2+} + 2Ni^{2+} + 3V^{5+} + 12O^{2-}$ is evaluated to be -2.18×10^{-4} emu mol-f.u.$^{-1}$ [16]. The Curie-Weiss θ is −16.4 K and about 2.27 times of T_N = 7.21 K. The magnitude of the effective magnetic moment μ_{eff} from the value of C = 2.60 K emu mol-f.u.$^{-1}$ is 3.23 μ_B Ni^{2+}-ion^{-1}, which is close to the spin only value 2.83 μ_B expected for S = 1, where the Lande's g-factor might be expected to be 2.28.

3.2.2 $AgCa_2Co_2V_3O_{12}$

The paramagnetic susceptibility χ of $AgCa_2Co_2V_3O_{12}$ over the temperature range 20 to 350 K does not obey the Curie-Weiss law as shown in Figs. 14 and 15. The susceptibility χ can not be described by one straight line over a wide temperature range. Here if we just pick up the experimental data for two temperature regions in Fig. 15, then we can obtain the fictitious (wrong) results as follows; (a) $20 \le T \le 60$ K : $\chi_0 = -2.95 \times 10^{-3}$ emu mol-f.u.$^{-1}$, θ = –23.0 K, C = 5.68 K emu mol-f.u.$^{-1}$, and μ_{eff} = 4.77 μ_B Co^{2+}-ion^{-1}, (b) $100 \le T \le 350$ K : $\chi_0 = -2.95 \times 10^{-3}$ emu mol-f.u.$^{-1}$, θ = –71.3 K, C = 8.66 K emu mol-f.u.$^{-1}$, and μ_{eff} = 5.88 μ_B Co^{2+}-ion^{-1}. The diamagnetic susceptibility by the atomic core orbital contribution χ_{dia} for $Ag^+ + 2Ca^{2+} + 2\,Co^{2+} + 3V^{5+} + 12O^{2-}$ is estimated to be $\chi_{dia} = -2.20 \times 10^{-4}$ emu mol-f.u.$^{-1}$ [16]. There is experimental uncertainty in the χ_0 although the value itself is small.

At first sight, these experimental results for the susceptibility of $AgCa_2Co_2V_3O_{12}$ may lead to an apparent interpretation that the high and low spin crossover takes place approximately 100 K where in the higher temperature μ_{eff} is 5.88 μ_B while 4.77 μ_B in the lower temperature. However, it should be noted that these values of the effective magnetic moment μ_{eff} are completely different from these magnitudes expected for 3.87 μ_B (S = 3/2 high spin state) and for 1.73 μ_B (S = 1/2 low spin state). In addition, the magnitude of the antiferromagnetic Weiss temperature θ = −71.3 K is too high in comparison with T_N = 6.39 K. The simple understanding on the basis of the Curie-Weiss law should be rejected. Consequently this simple interpretation is wrong. The authors would like to point out careful understanding and discussion as follows. These results are discussed in conjunction with the outstanding Tanabe-Sugano energy diagram based on the cubic crystalline electric field theory with the octahedral symmetry [17, 18]. The unified physical picture has been derived from the same discussion reported in Ref. [19] within the framework of Tanabe-Sugano energy diagram. Here we present the significant energy levels only around the ground state as shown in Fig. 16, which refers to the Tanabe-Sugano energy diagram of ref. [17, 18]. The crystalline electric field parameter Dq indicates the strength of CEF and B is Racah's parameter defined as the value of linear combination of Slater integrals introduced

grals introduced by Racah [17, 18]. The transition from the weak CEF with high spin state to the strong CEF with low spin state takes place for Co^{2+} ion at the vertical line of *Dq/B* ~2.17. The Rietveld analysis has been accomplished for $AgCa_2Co_2V_3O_{12}$ [14]. The result of $AgCa_2Co_2V_3O_{12}$ tells interesting result that the CoO_6-octahedron is firm and tight. The bond length between Co^{2+} and O^{2-} is 2.087(4) Å, which is extremely short and sufficient to provide the strong CEF. Presumably the same strong CEF takes place in the $AgCa_2Co_2V_3O_{12}$.

Our experimental results may indicate that the value of *Dq* for $AgCa_2Co_2V_3O_{12}$ is located at the just after the transition of from high spin to low spin state. Here *Dq/B* is ~2.3 just a little larger than *Dq/B* ~2.17. This Tanabe-Sugano energy diagram for d^7 configuration for Co^{2+} at *Dq/B* ~2.3 indicates that the energy level constructs from the ground state $^2E(t_2^6e)$ at the bottom to $^4T_1(t_2^5e^2)$, $^2T_1$, $^2T_2$, $^4T_2(t_2^4e^3)$, $^4T_1$, $^2A_1$, $^4A_2(t_2^3e^4)$, and the highest state of $^2A_2$. On the other hand, the energy levels for the free ion of Co^{2+} with *Dq/B* = 0 from the bottom ground state to the highest state are ^4F, ^4P, ^2G, ^2H, ^2P, ^2_aD, ^2F, and ^2_bD. In the influence of CEF, ^4F ground state splits into $^4T_1(t_2^5e^2)$, $^4T_2(t_2^4e^3)$ and $^4A_2(t_2^3e^4)$ and the second excited state ^2G plays an important role because ^2G state also splits under the influence of CEF. One of the split component of ^2G state is ^2E state which becomes the ground state in the strong CEF of value *Dq/B* larger than ~2.17. This ^2E state crosses all the quartet levels on its way down, as can be seen in the Tanabe-Sugano energy diagram, see Fig. 16.

The magnitude of *Dq/B* ~2.3 for $AgCa_2Co_2V_3O_{12}$ gives two significant levels of the ground state $^2E(t_2^6e)$ and the first excited state of $^4T_1(t_2^5e^2)$. The $^4T_1(t_2^5e^2)$ state is extremely close to $^2E(t_2^6e)$ state and a little higher than that. We can not neglect the thermally accessible occupation of the excited state $^4T_1(t_2^5e^2)$ for the interpretation of the magnetic susceptibility.

Here let us take a next step. It is unable for us to pursue a quantitative analysis of the susceptibility because of the many unknown parameters in the crystalline electric field theory. Therefore we try a feasible approach where the basic view point from the Tanabe-Sugano energy diagram is maintained. We introduce an effective magnetic moment p_{eff} which is expressed by [20],

$$p_{\mathrm{eff}} = \frac{1}{\mu_{\mathrm{B}}}\sqrt{\frac{3k_{\mathrm{B}}(\chi-\chi_0)T}{N}} \quad , \tag{10}$$

here χ is the experimental value of the temperature dependent magnetic susceptibility, k_{B} the Boltzmann's constant, μ_{B} the Bohr magneton and N the number of magnetic ion. Temperature dependence of p_{eff} per magnetic ion is shown in Figs. 17 and 18. For $AgCa_2Ni_2V_3O_{12}$, Fig. 17 indicates the same values of $\chi(T)$ as these obtained in Fig. 14 for a comparison. The straight and horizontal line is seen over the wide temperature range over 50 to 300 K in $AgCa_2Ni_2V_3O_{12}$ as shown in Fig. 17, which supports the applicability of the Curie-Weiss law. Nevertheless, $AgCa_2Co_2V_3O_{12}$ demonstrates the curved line for p_{eff} as seen in Fig. 18. We note that the measured value of $\chi(T)$ includes the temperature independent Van Vleck paramagnetic contribution in addition to the stated diamagnetic core contribution χ_0 and/or appreciable experimental errors, then we must subtract before being compared with theoretical results. Fig. 18 shows the χ_0 dependence of p_{eff} as a function of temperature. Any magnitude of χ_0 does not fulfill and reproduce a straight and horizontal line. The complex temperature dependence of the susceptibility is reflected in the performance of p_{eff}, which origi-

nates from the existence of the first excited spin quartet $^4T_1(t_2^5e^2)$ state just a bit higher than the ground spin doublet $^2E(t_2^6e)$ state. Consequently two magnetic states with $S = 3/2$ and $S = 1/2$ are excited and active magnetically at higher temperature. It should be noticed that our model does not mean the simple high ($S = 3/2$) to low spin state ($S = 1/2$) transition, but the z-component S_z of spin is 6, because +1/2, -1/2 from ground state and +3/2, +1/2, −1/2, and −3/2, so that this value corresponds effectively (not exactly) to $S = 5/2$ where the presence of a thermally accessible spin 3/2 excited. The above analysis has been treated within the framework of the Tanabe-Sugano theory.

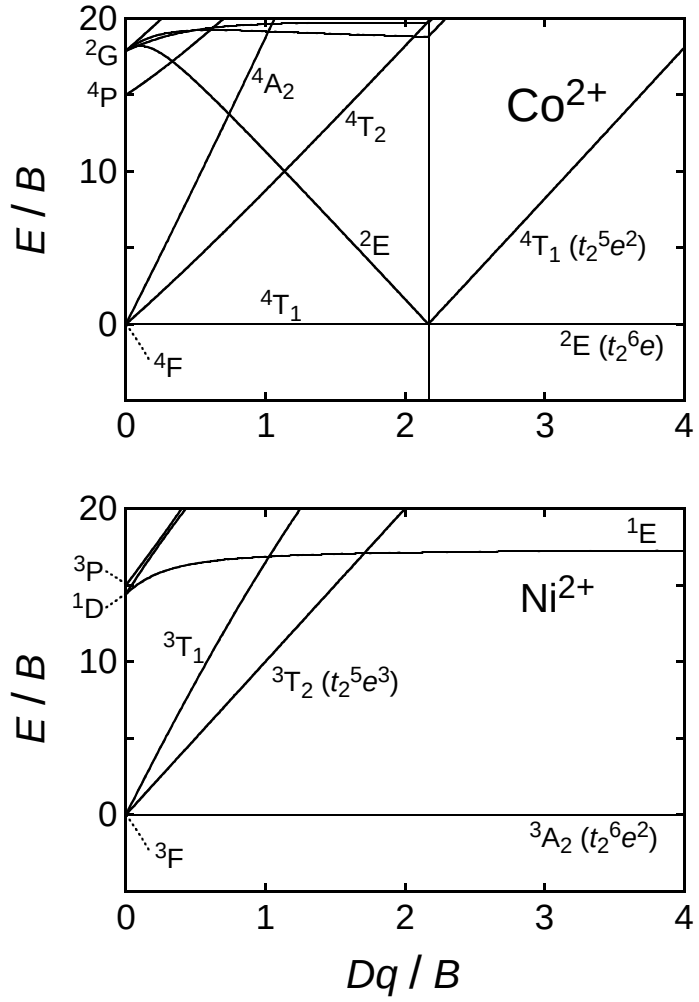

Fig. 16. The energy diagram close to the ground state which is referred to as the Tanabe-Sugano energy diagram based on the cubic crystalline electric field theory with the octahedral symmetry. The level energy (ordinate) is measured from the ground state and the strength of the crystalline electric field (abscissa) is scaled by B as unit, see text and Refs. [17 ,18].

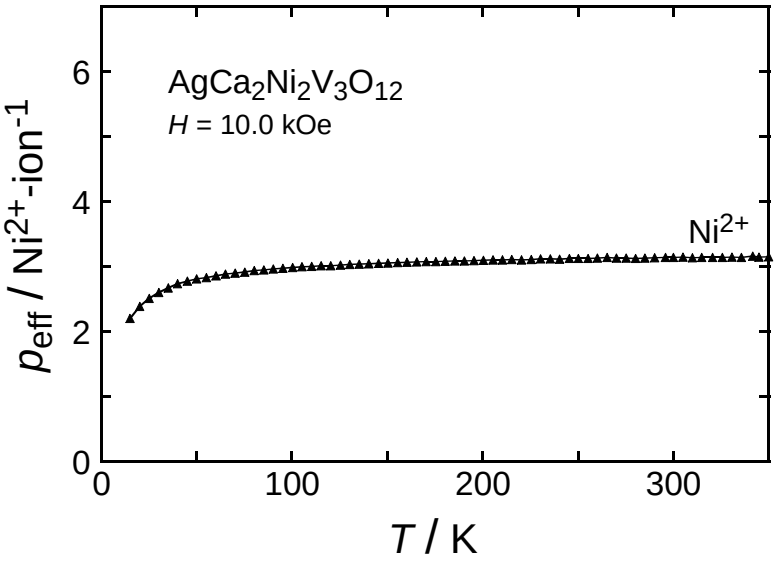

Fig. 17. The effective magneton number of Ni^{2+} ion in $AgCa_2Ni_2V_3O_{12}$ as a function of temperature; $\chi_0 = 3.16 \times 10^{-3}$ emu mol-f.u.$^{-1}$.

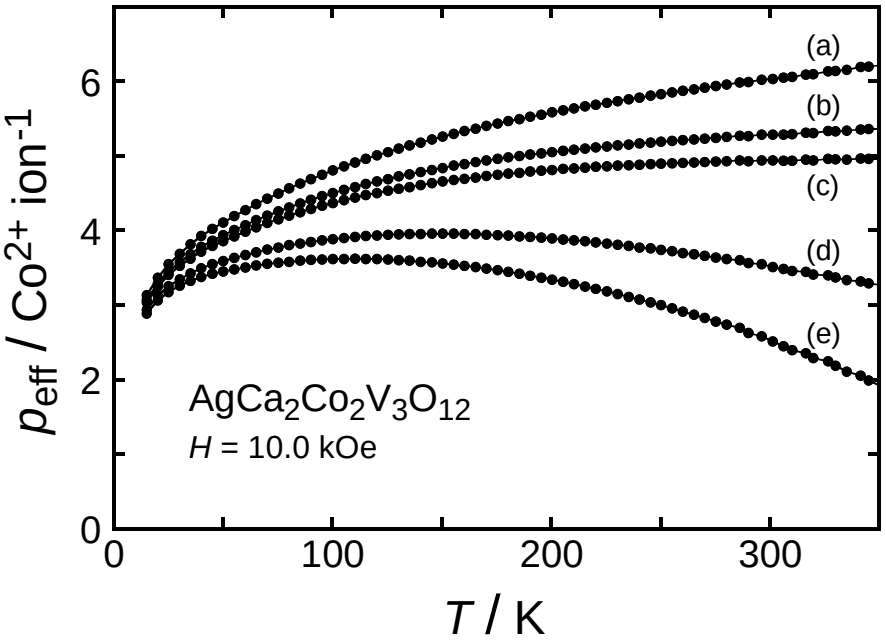

Fig. 18. The variation of the effective magneton number of Co^{2+} ion in $AgCa_2Co_2V_3O_{12}$ on the magnitude of χ_0: (a) $\chi_0 = -1.00 \times 10^{-2}$ emu mol-f.u.$^{-1}$, (b) $\chi_0 = -2.95 \times 10^{-3}$ emu mol-f.u.$^{-1}$, (c) $\chi_0 = 0.00$ emu mol-f.u.$^{-1}$, (d) $\chi_0 = 1.00 \times 10^{-2}$ emu mol-f.u.$^{-1}$, (e) $\chi_0 = 1.50 \times 10^{-2}$ emu mol-f.u.$^{-1}$.

It should be noted, nevertheless, that the other nice route to reach the Co^{2+} problem in the octahedral field on the basis of the spin-orbit coupling [21], and the spin Hamiltonian method [22]. Here we have omitted the detailed discussion on the basis of these theories, see Ref. [19, 21, 22]. We point out that many previous researchers experienced a severe struggle for understanding the magnetic susceptibility for the almost same structure of vanadium garnet $NaCa_2Co_2V_3O_{12}$ [3, 5, 10] and $NaPb_2Co_2V_3O_{12}$ [19]. The garnet structure contains CoO_6 octahedron at the *A*-site of Co^{2+} ion which has extremely rigid. Consequently, Co^{2+} ion is strongly influenced by the CEF of O^{2-} ions. These difficulty can be removed by the existence of excited spin quartet state $^4T_1(t_2^5e^2)$ just a little bit higher than ground spin doublet state $^2E(t_2^6e)$ state, on the basis of CEF theory. Fig. 16 predicts also that the electron configuration d^8 for Ni^{2+} ion in the cubic CEF with octahedral symmetry does not cause the transition from high to low spin state when the CEF strength parameter *Dq* varies from weak to strong. The ground state of d^8 for Ni^{2+} ion in the cubic CEF maintains the spin triplet state $^3A_2(t_2^6e^2)$ with any changing the value of *Dq*, furthermore, the excited states of the energy levels in the cubic CEF are rather higher than that of the ground sate. Therefore the spin triplet state is fairly defined. These situation guarantees the applicability of the Curie-Weiss law to the magnetic susceptibility data of $AgCa_2Ni_2V_3O_{12}$. Consequently, all the experimental results give the reasonable magnitudes expected.

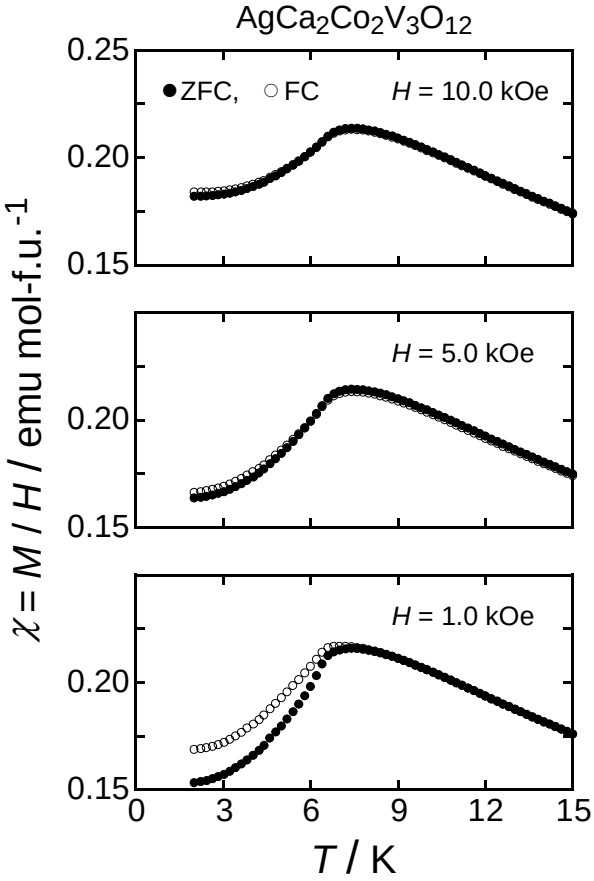

Fig. 19. Magnetic susceptibility of $AgCa_2Co_2V_3O_{12}$ as a function of temperature in three magnetic fields of 10.000 kOe, 5.000 kOe and 1.000 kOe under ZFC and FC conditions.

3.2.3 *Field dependence of the susceptibility below T_N*

Figs. 19 and 20 provide the magnetic field dependence magnetic susceptibility on emphasizing the temperature region below T_N. The difference between field-cooled ($\chi_{FC} = M_{FC}/H$) and zero-field-cooled ($\chi_{ZFC} = M_{ZFC}/H$) susceptibility decreases with increasing field as can be seen in Figs. 19 and 20. This characteristic feature was found in both of $AgCa_2Co_2V_3O_{12}$ and $AgCa_2Ni_2V_3O_{12}$. The deviation of χ_{FC} from χ_{ZFC} starts higher temperature with decreasing field.

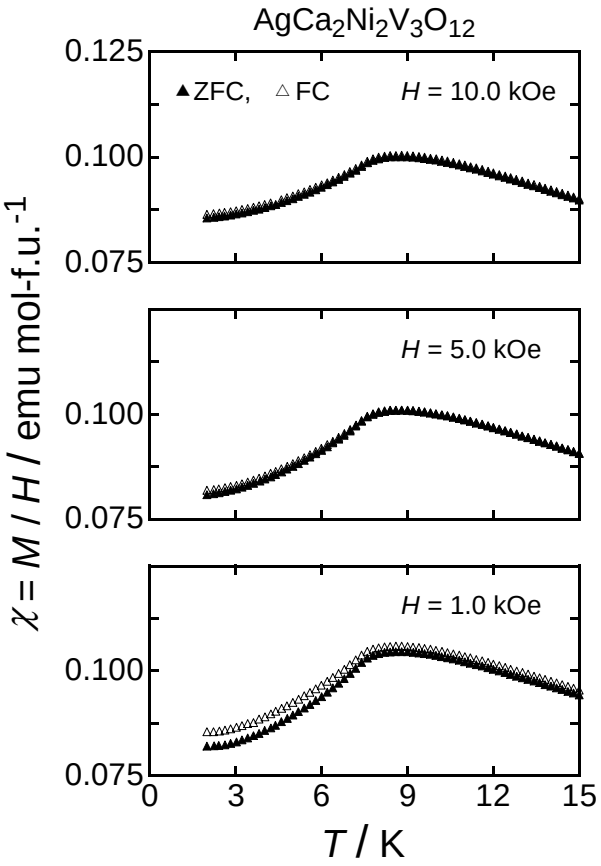

Fig. 20. Magnetic susceptibility of $AgCa_2Ni_2V_3O_{12}$ as a function of temperature in three magnetic fields of 10.000 kOe, 5.000 kOe and 1.000 kOe under ZFC and FC conditions.

4. Acknowledgements

The authors would like to thank Mr. K. Hashimoto and Mr. T. Mizuuchi for their helpful experimental collabortion. The athors would like to thank Dr. S. Ebisu and Professor S. Chikazawa for kind discussion.

References

[1] S. Geller, Z. Krist, **125** (1967) 1.
[2] J. P. Vorobev *et al.*, Perspekt. Mater. (Russ.) **2** (1998) 39.
[3] M. T. Korayem, Indian J. Phys. **67A** (1993) 53.
[4] B. Blanzat, J. Loriers, Mat. Res. Bull. **9** (1974) 1647.
[5] V. I. Sokolov, H. Szymczak, W. Wardzynski, Phys. Status. Sol.(b) **55** (1973) 781.
[6] G. Ronninger, B. V. Mill, V. I. Sokolov, Kristallografia **19** (1974) 361.
[7] E. L. Dukhovskaya, B. V. Mill, Kristallografia **19** (1974) 84.
[8] I. V. Golosovsky, V. P. Plakhty, B. V. Mill, V. I. Sokolov, O. P. Shevaleevsky, Solid State Commun. **14** (1974) 309.
[9] G. Ronniger, B. V. Mill, Soviet Phys. Cryst. (English Transl.) **18** (1973) 339.
[10] R. P. Ozerov, N. V. Fadeeva, JETP Ltters (English Transl.) **16** (1972) 198.
[11] V. P. Plakhtii, I. V. Golosovskii, V. A. Duryashev, O. P. Smirnov, JETP Ltters (English Transl.) **16** (1972) 194.
[12] K. P. Belov, B. V. Mill, G. Ronninger, V. I. Solokov, T. D. Hien, Soviet Phys. (Solid State). **12** (1970) 1393.
[13] J. M. Desvignes, P. Feldmann, H. Le Gall, J. Cryst. Growth **52** (1981) 650.
[14] J. Awaka, N. Kijima, M. Uemura, Y. Kawashima, S. Nagata, J. Phys. Chem. Solids **66** (2005) 103 .
[15] J. Awaka, R. Katagi, H. Sasaki, R. Endoh, N. Matsumoto, S. Ebisu, S. Nagata, J. Phys. Chem. Solids **62** (2001) 743.
[16] K. H. Hellwege, A. M. Hellwege (Eds.), Landolt-Börnstein, Group II, vol. **8**, Springer, Berlin, 1976, p. 27.
[17] Y. Tanabe, S. Sugano, J. Phys. Soc. Jpn **9** (1954) 753.
[18] Y. Tanabe, S. Sugano, J. Phys. Soc. Jpn **9** (1954) 766.
[19] S. Nagata, T. Yamagishi, K. Awaka, J. Awaka, J. Phys. Chem. Solids **66** (2005) 177.
[20] M. Kotani, Prog. Theor. Phys. (Supplement) **14** (1960) 1.
[21] W. Low, Phys. Rev. 109 (1958) 256.
[22] A. Abragam and M. H. L. Pryce, Proc. Roy. Soc. A205 (1951) 135.